Computer-assisted mesh generation based on Hydrological Response Units for distributed hydrological modelling

P. Sanzana Cuevas, S. Jankowfsky, F. Branger, Isabelle Braud, X. Vargas, N. Hitschfeld, J. Gironas

Author-produced version of the article published in Computers & Geosciences, 2013, vol. 57
The original publication is available at http://www.sciencedirect.com/
doi:10.1016/j.cageo.2013.02.006

Computer-assisted mesh generation based on Hydrological Response Units for distributed hydrological modelling

P. Sanzana*[1,2,5], S. Jankowfsky[1], F. Branger[1] , I. Braud[1], X. Vargas[2], N. Hitschfeld[3], J. Gironás[4]

[1]Irstea, UR HHLY (Hydrology- Hydraulics), 3bis Quai Chauveau, CP 220, 69336 Lyon Cedex 9, France.

[2] Departamento de Ingeniería Civil, Facultad de Ciencias Físicas y Matemáticas, Universidad de Chile, Blanco Encalada 2002, Santiago, Chile.

[3] Computer Science Department, Facultad de Ciencias Físicas y Matemáticas, Universidad de Chile. Av. Blanco Encalada 2120, Santiago, Chile.

[4] Departamento de Ingeniería Hidráulica y Ambiental, Pontificia Universidad Católica de Chile, Av. Vicuña Mackenna 4860, Santiago, Chile.

[5]Centro de Estudios Avanzados en Zonas Áridas (CEAZA), Raúl Bitrán s/n, Campus Andrés Bello, Colina El Pino s/n, La Serena, Chile.

*Corresponding Author: pedro.sanzana@ceaza.cl, Telephone: 56-51-204378, Fax: 56-51-334874. Mailbox: Casilla 599, Correos de Chile.

Author-produced version of the article published in Computers & Geosciences, 2013, vol. 57
The original publication is available at http://www.sciencedirect.com/
doi:10.1016/j.cageo.2013.02.006

Abstract

Distributed hydrological models rely on a spatial discretization composed of homogeneous units representing different areas within the catchment. Hydrological Response Units (HRUs) typically form the basis of such a discretization. HRUs are generally obtained by intersecting raster or vector layers of land uses, soil types, geology and sub-catchments. Polylines maps representing ditches and river drainage networks can also be used. However this overlapping may result in a mesh with numerical and topological problems not highly representative of the terrain. Thus, a pre-processing is needed to improve the mesh in order to avoid negative effects on the performance of the hydrological model. This paper proposes computer-assisted mesh generation tools to obtain a more regular and physically meaningful mesh of HRUs suitable for hydrologic modelling. We combined existing tools with newly developed scripts implemented in GRASS GIS. The developed scripts address the following problems: (1) high heterogeneity in Digital Elevation Model derived properties within the HRUs, (2) correction of concave polygons or polygons with holes inside, (3) segmentation of very large polygons, and (4) bad estimations of units' perimeter and distances among them. The improvement process was applied and tested using two small catchments in France. The improvement of the spatial discretization was further assessed by comparing the representation and arrangement of overland flow paths in the original and improved meshes. Overall, a more realistic physical representation was obtained with the improved meshes, which should enhance the computation of surface and sub-surface flows in a hydrologic model.

KEYWORDS: GRASS GIS, Hydrological Response Units, Distributed hydrological model, Computer-assisted Mesh Generation, Terrain representation.

Author-produced version of the article published in Computers & Geosciences, 2013, vol. 57
The original publication is available at http://www.sciencedirect.com/
doi:10.1016/j.cageo.2013.02.006

1. Introduction

Distributed hydrological models represent the catchment heterogeneity in an explicit way. Thus, a discretization leading to homogeneous and representative spatial units becomes relevant to solve the equations describing the physical processes involved. Pixels in a grid-cell representation are the elementary spatial units mostly used by many models such as the Système Hydrologique Européen model (Abbott et al., 1986a, 1986b) or TOPMODEL (Beven and Kirkby, 1979) to represent spatial information. Other models consider a vector objects representation in which a non-uniform mesh of elementary irregular units is defined. The Hydrological Response Unit (HRU), concept proposed by Flügel (1995), is an example of these elementary units. HRUs possess unique land uses, soil attributes and flow routing properties, which are derived from intersecting polygon layers representing information such as land use, soil type, sub-catchments and geology. Polyline layers corresponding to natural and artificial drainage elements can typically be combined with a HRU representation. Thus, the resulting hydrological mesh is formed by simple polygons with very irregular shapes, which are more suitable for representing man-made features that significantly affect hydrological processes in a catchment (Lagacherie et al., 2010). This is particularly relevant for suburban and urban catchments, in which artificial elements (i.e. sewers, channels and streets) can modify significantly the flow directions (Gironás et al., 2009). Some of the distributed hydrological models based on a HRU representation include PRMS (Flügel, 1995; Bongartz, 2003), SWAT (Arnold et al., 1998), J2000 (Krause, 2002), MHYDAS (Moussa et al., 2002), PREVAH (Viviroli et al., 2009), and models built within the LIQUID modelling framework (Branger et al., 2010).

Author-produced version of the article published in Computers & Geosciences, 2013, vol. 57
The original publication is available at http://www.sciencedirect.com/
doi:10.1016/j.cageo.2013.02.006

For the determination of non-uniform meshes of elementary units, Dehotin and Braud (2008) proposed a three level discretization methodology: i) Catchment sub-divided into sub-catchments, ii) sub-catchments discretized into hydro-landscapes (e.g. HRUs) where hydrological processes are homogeneous, and iii) hydro-landscapes further adapted to fulfil numerical constraints. This paper addresses this third level and some aspects of the second level.

Several GIS tools have been developed to delineate HRUs, including GRASS-HRU (Schwartze, 2008), Geo-MHYDAS (Lagacherie et al., 2010), WINHRU and GRIDMATH (Viviroli et al., 2009), and AVSWAT (Di Luzio et al., 2004). However, vector based HRU model meshes come also with specific constraints. Special considerations regarding topological and geometric characteristics of the HRUs are needed to obtain stable and meaningful numerical solutions. The three main issues to be addressed when defining HRUs are:

1. Cleaning of polygon geometry and topology to deal with:

a) The direct overlay of several digitized polygons or lines layers can create small artificial non-representative units, which play no role in representing the terrain and must be dissolved. As an example Fig. 1a shows an isolated small artificial unit generated near a major unit (Fig. 1b). When numerous, these units can increase the computation time.

b) Digitalization of raster images can create polygons with many right angles representing the size of the grid cell. The length of the polygon boundary, often used for calculating wetted sections in overland and subsurface flow, becomes longer in this case. Hence,

Author-produced version of the article published in Computers & Geosciences, 2013, vol. 57
The original publication is available at http://www.sciencedirect.com/
doi:10.1016/j.cageo.2013.02.006

the perimeter of these polygons should be smoothed to avoid overestimation of boundary lengths (Fig. 1b).

c) Polygon intersections can create holes inside the HRUs, generating numerical indefinition in the hydrological model (Fig. 1d). These units must be partitioned to avoid the generation of these holes and properly connect HRU's to ensure continuity in the model.

2. Improving the property homogeneity within a model unit.

Topography partly controls water fluxes within a watershed and influences many aspects of the hydrologic system (Wolock and Price, 1994). Thus, raster based information such as elevation or slope, is of interest for simulating hydrological processes. As this information is not initially included in the HRUs definition, these properties may not be homogeneous enough within a given HRU, and further segmentation may be necessary to get more homogeneous units.

3. Improving the mesh geometry for a better numerical stability.

Land use objects, such as forest stretches, hedgerows, agricultural fields or urban cadastral units do not always have convex geometries. Furthermore, the overlay of different property layers can create bad-shaped polygons with thin geometries (Fig. 1b) or polygons with their centroid outside of their boundary (Fig. 1c). This may cause problems when defining the topology of flow routing from one HRU to another. Typically, the distance between the centroids of the polygons and their boundaries is used to calculate flow path lengths among HRUs and overland and subsurface flows. This distance has no realistic meaning if the centroid is outside of the polygon, and a modification of the HRUs becomes necessary.

Author-produced version of the article published in Computers & Geosciences, 2013, vol. 57
The original publication is available at http://www.sciencedirect.com/
doi:10.1016/j.cageo.2013.02.006

Finally, HRUs can greatly vary in sizes, which can affect flow routing and the stability of numerical schemes. Thus, the segmentation of very large polygons is recommended to obtain a more homogeneous model mesh.

< Figure 1 >

Cleaning tools available in most GIS software can solve the first category of issues. To address situation 1a in GRASS (GRASS Development Team, 2011), Schwartze (2008) used raster pixel-dissolving functions and generated vector HRUs using a raster-to-vector conversion. Alternatively, Lagacherie et al. (2010) developed enhanced dissolving tools for vector data in GeoMHYDAS, which are specific to HRUs. Problem 1b can be solved using specific GIS functions such as the m.douglas tool (Lagacherie et al., 2010), based on the Douglas-Peucker algorithm (Douglas and Peucker, 1973), or the Snakes algorithm (Kass et al., 1988) of the function v.generalize in GRASS. Problem 1c must be addressed with a segmentation approach. Most common partition algorithms transform polygons into simpler polygons such as trapezoids or triangles. However these algorithms increase the number of final polygons and the mesh units become physically meaningless.

The second category of issues relates to the heterogeneity typically represented by raster data. The grid resolution must be small enough to describe this variability (Seyfried and Wilcox, 1995), particularly if this is significant. For example, Zhang and Montgomery (1994) found that a 10 m grid resolution allowed a good compromise between the quality of the terrain representation and data volume for simulating physical processes. To analyse terrain heterogeneity GRASS has comprehensive tools described by Hofierka et al. (2007). TOPAZ uses automated analysis of digital landscape topography in raster scheme, as

Author-produced version of the article published in Computers & Geosciences, 2013, vol. 57
The original publication is available at http://www.sciencedirect.com/
doi:10.1016/j.cageo.2013.02.006

described by Garbrecht and Martz (1997). However, these tools cannot be applied to analyse raster-based terrain properties within polygons derived from vectorial layers.

The third category of issues is more complex. Lagacherie et al. (2010) proposed an algorithm for sliver areal features, which dissolves thin polygons with their neighbours. Sometimes this approach is not desirable, as the bad-shaped polygon may correspond to a relevant hydrological object. An alternative approach is to sub-discretize the HRUs into Triangular Irregular Networks (TINs) (Bocher and Martin, 2012). TIN meshes are well adapted to numerical solutions of differential equations, and are used in comprehensive hydrological models such as InHM (VanderKwaak and Loague, 2001) or tRIBS (Ivanov et al., 2004). This approach also increases the number of model units, and the physiographical character of the mesh also gets lost.

The objective of our study was to generate an HRU model mesh compatible with numerical criteria and homogeneity requirements. We developed mesh generation computer assisted tools addressing the problems mentioned above, focusing more specifically on problems listed in category 2 and 3. Although our work is a contribution to the development of the hydrologic peri-urban PUMMA Model (Jankowfsky et al., 2010, Jankowfsky, 2011), built within the LIQUID modelling framework (Branger et al., 2010), the concepts and methods involved are also relevant for other distributed hydrological models. These methods and concepts can be applied to models in which interconnected HRUs are generated from objects typically found in periurban catchments, such as urban cadastral units, agricultural fields and forests, and artificial and natural drainage systems. A central objective in our development is to better represent overland and subsurface flow paths, as well as interactions with the natural and artificial drainage network. This improvement allows the

Author-produced version of the article published in Computers & Geosciences, 2013, vol. 57
The original publication is available at http://www.sciencedirect.com/
doi:10.1016/j.cageo.2013.02.006

155 understanding and quantification of runoff contributions from a variety of HRU's to the
156 different components of drainage networks.

157 ## 2. Materials and methods

158 In this section, we first review the data preparation methods to obtain clean and
159 topologically consistent GIS layers. Then the following new methods to improve the model
160 mesh are presented in detail: (1) segmentation of polygons with high variability of a given
161 property, (2) removal of bad-shaped polygons, and (3) segmentation of very large
162 polygons. Finally, we present the case study catchments used to test the proposed methods.

163 We developed several Python (Python Software Foundation, 2011) scripts to implement
164 these new methods (Table 1). The scripts include GRASS GIS functions, as GRASS is the
165 only free open-source GIS software with topological functionalities (Branger et al., 2012).
166 Additional software such as Triangle (Shewchuck, 1996) and R (R development Core
167 Team, 2011), were also used to get fast and high quality triangulation of bad-shaped
168 polygons. The developed tools are computer- assisted because, although they strongly rely
169 on computer coding, the modeller must still provide critical information such as threshold
170 values, ranges and specific quantities for the complete execution. Similar computer
171 algorithms in which the user must provide specific information are widely used. For
172 example, threshold values for contributing areas are needed for channel identification in
173 DEM's when using tools such as r.watershed in GRASS or Arc-Hydro in Arc-GIS (Olivera
174 et al., 2002). Furthermore, quantity and ranges of slope, aspect and height contours are
175 required in the overlapping delineation processes proposed by Schwartze (2008) to generate
176 HRUs. Finally, the segmentation procedure implemented in GeoMHYDAS (Lagacherie et
177 al., 2010) requires a minimum area to dissolve neglected and sliver units.

Author-produced version of the article published in Computers & Geosciences, 2013, vol. 57
The original publication is available at http://www.sciencedirect.com/
doi:10.1016/j.cageo.2013.02.006

<Table 1>

2.1 Data preparation and cleaning of GIS layers: smoothing and partition of polygons with holes

Typically a pre-processing is required before each segmentation task to obtain "clean" layers. For the smoothing of boundaries, the Douglas-Peucker (Douglas and Peucker, 1973) and Snakes (Kass et al, 1988) algorithms were assessed. Two implementations of the Douglas-Peucker algorithm are available in GRASS: the command v.generalize and the script m.douglas (Rabotin, 2010).

The intersection of different layers can lead to polygons inside external polygons, referred as to holes, which are undesirable for spatial modelling as they can distort flow paths. The implemented algorithm (*polygons_holes.py* in Table 1) subdivides all polygons with holes to generate new sub-sets of polygons without them (Fig. 2). The algorithm first identifies the shortest distance from each vertex of the inner polygon to the outer polygon (*w*, *x*, *y* and *z* in Fig. 2). Then the shortest and longest distances, *x* and *z*, are used to generate the polylines to split the outer polygon and transform the hole in a new polygon.

< Figure 2>

2.2 Segmentation of polygons with high variability of a raster-based property: application with slope criterion

For hydrologic modelling, it is desirable to incorporate some raster-based properties not included in the initial HRU delineation. An example of such property is the slope, which is typically available in a grid-cell representation, and affects different relevant hydrological

Author-produced version of the article published in Computers & Geosciences, 2013, vol. 57
The original publication is available at http://www.sciencedirect.com/
doi:10.1016/j.cageo.2013.02.006

processes. Hence, a further segmentation process is necessary to disaggregate highly heterogeneous HRUs into regions with homogeneous features. For this purpose, we used a threshold value of the standard deviation of the property (σ_T). For values of standard deviation $\sigma > \sigma_T$, segmentation is performed. The threshold could also be defined in terms of the coefficient of variation, in order to compare polygons with different mean values of the property. However, by using σ_T one can control the allowable dispersion within each polygon. To define the boundaries delimiting homogeneous property areas within the different HRUs, we used the Inter Quartile Range (IQR), a statistical parameter defined as the difference between the third and first quartiles (Q3) and (Q1). The segmentation procedure is defined in details in the Appendix A.1 and illustrated in Fig. 3 using the slope as the raster-based property.

< Figure 3>

2.3 Segmentation of concave units

The flowpath length between HRUs is given by the distance between their geometric centroids. Hence, this distance must be representative of the trajectory to get a realistic physical description of the flow. Therefore the partition of bad-shaped polygons becomes necessary to obtain convex or pseudo-convex polygons with their geometric centroid located within them.

Well-shaped polygons (Fig. 4a) facilitate the definition of a meaningful length in contrast to bad-shaped polygons (Fig. 4b, 4c, 4d). The identification and correction of these polygons is then required. Different shape descriptors proposed by Russ (2002), such as the Form Factor ($FF = (4\pi A) / P^2$), Compact ($C = \sqrt{4\pi A} / P$), Solidity Index ($SI = A / A_{Convex}$)

Author-produced version of the article published in Computers & Geosciences, 2013, vol. 57
The original publication is available at http://www.sciencedirect.com/
doi:10.1016/j.cageo.2013.02.006

and Convexity Index ($CI = P_{Convex}/P$), can be used for identifying well- and bad-shaped polygons. In these descriptors, P and A are the perimeter and area of the polygon, and P_{Convex} and A_{Convex} are the perimeter and area of the convex hull polygon containing the polygon of interest. The convex hull area is the minimal convex area in which any line between two inner points is completely contained within the polygon. A convex polygon always has its geometrical centroid inside and can be considered as a well-shaped unit.

Each descriptor characterizes different geometrical features (Fig. 4). For example, *FF* and *C* are sensitive to thin units (i.e. values of these descriptors decrease for $A << P$), whereas *CI* and *SI* are sensitive to concave polygons, focusing on the perimeter and the area respectively. *SI* is inversely proportional to the convex-hull area, as shown in Fig. 4b (SI = 0.616) and Fig. 4c (SI = 0.388). As *CI* detects best concave polygons, (i.e. polygon in Fig. 4d), a Convexity Index Threshold (*CIT*) was chosen for the identification of the polygons requiring correction. Values of $CI < CIT$ are associated with bad-shaped polygons that must be corrected.

< Figure 4>

Some algorithms are available for partitioning polygons into convex pieces, with the triangulation being the simplest one, although non-optimal in terms of the number of convex pieces generated (O´Rourke, 1998). The Hertel and Mehlhorn algorithm (Hertel and Mehlhorn, 1983) provides a simple and fast solution that does not minimize the number of pieces. It arbitrarily triangulates the polygon and deletes the diagonal to generate only convex polygons. On the other hand, the Greene Algorithm (Greene, 1983) available in the CGAL Library (CGAL, 2011) generates the minimum number of pieces, but is more time

Author-produced version of the article published in Computers & Geosciences, 2013, vol. 57
The original publication is available at http://www.sciencedirect.com/
doi:10.1016/j.cageo.2013.02.006

consuming (O'Rourke, 1998). With both algorithms, the number of final pieces depends on the number of vertexes of the input polygons, and computation cost can become a relevant issue both in the generation of the improved mesh and the subsequent hydrologic modelling.

The GRASS function v.delaunay, creates a Delaunay triangulation from an input vector map, although it is not a robust implementation and works only with convex polygons. Hence, our solution considers first a Delaunay triangulation using the *Triangle* Software (Shewchuck, 1996) which can address concave or convex polygons, with or without holes. Second, we dissolve adjacent triangles based on a chosen value of the *CIT* (Fig. 5) to decrease the number of polygons and improve the physical meaning of each unit of the model mesh. The dissolution rule takes into account the *CI* with a hierarchical area order. Triangles are dissolved so that the *CI* values of all new generated polygons equal or exceed the *CIT* value. The convex segmentation procedure is defined in the Appendix A.2 and illustrated in Fig. 5 using a *CIT* value of 0.95. The final number of pseudo-convex pieces depends on the *CIT* value. For instance, in the example of Fig. 5, the number of final pieces decreases to 2 when *CIT* equals 0.90.

< Figure 5>

2.4 Segmentation of very large polygons

Large polygons generate numerical problems when connected to small polygons. This can affect the calculation of flow paths, water fluxes, ponding levels or water table levels. All the polygons with an area exceeding a threshold value defined by the user are segmented

Author-produced version of the article published in Computers & Geosciences, 2013, vol. 57
The original publication is available at http://www.sciencedirect.com/
doi:10.1016/j.cageo.2013.02.006

with the same procedure used for the convexity segmentation that considers a maximum triangle area in the triangulation.

2.5 Case study

The computer-assisted mesh generation tools were tested in two subcatchments within the Yzeron peri-urban watershed (150 km^2) located south west of Lyon, France (Fig. 6). The Mercier subcatchment (7 km^2) is covered with forests, crops and urban areas (about 10%), while the Chaudanne subcatchment (4.1 km^2) is covered by a mix of crops (45%) and urbanized areas (53 %) (Braud et al., 2012). Given that most of the issues previously depicted are typically related to polygons generated in rural areas, we focused our analysis on the Mercier catchment. Nonetheless we also provide some representative statistics for the Chaudanne catchment.

< Figure 6 >

HRUs were delineated from several maps including a detailed land use map obtained by manual digitalization (Jacqueminet et al., 2013), a pedology map produced by the Soil Information of Rhône-Alpes as part of the Soil Management, Conservation and Inventory program (IGCS, 2013), a geology map (BRGM, 2013), a 2 m resolution Digital Elevation Model (DEM) derived from a Lidar (Light Detection And Ranging) survey (Sarrazin, 2012), a subcatchment map derived using the method proposed by Jankowfsky et al. (2012), maps of the ditch network (Jankowfsky et al., 2012), as well as sewer maps, which were provided by the local sewer system manager SIAHVY (Syndicat Intercommunal pour l'Aménagement de la Vallée de l'Yzeron). The HRU map derived from the rough intersection of all these layers is shown in Fig. 7a.

Author-produced version of the article published in Computers & Geosciences, 2013, vol. 57
The original publication is available at http://www.sciencedirect.com/
doi:10.1016/j.cageo.2013.02.006

< Figure 7>

3. Results

This section describes the results obtained when applying each of the steps of the improvement procedure previously described, as well as the issues found in generating the physiographical representation for the study subcatchments. Although not compulsory, we recommend applying these steps in the same order as shown. Jankowfsky (2011) provides more details and results when using the proposed sequence in the Mercier and Chaudanne catchments.

3.1 Data preparation and cleaning of GIS layers

One of the main problems detected at initial stages was the non-representative shapes of areas with vegetation, whose extraction is affected by the low resolution of the corresponding raster images. Thus, the perimeter of these shapes is originally overestimated (Fig. 8a). After trying both the Douglas-Peucker algorithm (Fig. 8b) and Snakes algorithm (Fig. 8c), we concluded that the last produces a more realistic representation and reduces the initial perimeter in about 25%.

< Figure 8 >

A second issue addressed at early stages was that of the holes within polygons. They were successfully segmented using the *polygons_holes.py script*, 10 in the Mercier and 11 in Chaudanne catchment. Fig. 9a and Fig. 9b show two HRUs partitioned to avoid the holes produced by two different vegetal features. Fig. 9c shows a HRU partitioned to avoid the hole produced by a greenhouse.

Author-produced version of the article published in Computers & Geosciences, 2013, vol. 57
The original publication is available at http://www.sciencedirect.com/
doi:10.1016/j.cageo.2013.02.006

< Figure 9>

3.2 Segmentation of polygons with high variability of a given property

We applied the proposed algorithm for the slope map of the Mercier catchment, which was obtained from the DEM using the r.slope function in GRASS. After a visual inspection of the Mercier HRUs, we chose a σ_T value of 6% for the slope. Fig. 3f shows the results obtained after applying the segmentation script *slope_segmentation.py* (Table 1). The IQR criterion generated new polygons whose boundaries had right angles. The subsequent application of the Douglas-Peucker and Snakes algorithms allowed reducing the vertexes and smoothing the contours, respectively. 42 polygons were segmented into 133 final pieces in the Mercier catchment. As a result the area covered by HRUs with high standard deviation was reduced from 93.4 ha to 51.6 ha, that means a reduction of 13% to 7% of the total area.

Furthermore, the integration of raster based properties into polygons allows segmenting units with a high standard deviation and creating new units. The final standard deviations of the new units depend on the spatial distribution of the parameter selected. Thus the script reduces the area covered by units with non-homogeneous distribution, but this does not assure that all the output units preserve a standard deviation less than the threshold (i.e. Maximum Standard deviation of Slope increase to 14.25 in Table 2). A possible solution to assure a reduction of the maximum value would be continuing segmenting in an iterative way, but this might result in very small units depending on the quality of the raster resolution. Overall, this segmentation method uses simple steps and produces satisfactory results, comparable to those generated by other more sophisticated methods (Klingseisena

Author-produced version of the article published in Computers & Geosciences, 2013, vol. 57
The original publication is available at http://www.sciencedirect.com/
doi:10.1016/j.cageo.2013.02.006

et al., 2008, Taylor et al., 2009), which can be also explored to potentially improve the resulting shapes from our method.

3.3 Segmentation of bad-shaped polygons

Polygons with *CI* less than a certain *CIT* were considered as bad shape units not suitable for modelling. Values of *CIT* = 0.75 and 0.88 were adopted for the Mercier catchment and the Chaudanne catchment, respectively. We chose different *CIT* values because of the available land-use maps. In the Chaudanne catchment the vegetation extracted from raster maps had a more detailed perimeter than in the Mercier catchment, for which the land use map was determined manually. Therefore, meshes with sinuous HRUs required a larger *CIT* value in order to obtain well-shaped elements. The convexity segmentation procedure previously depicted was applied to all the HRUs using these *CIT* values. 20 polygons within the Mercier catchment were modified. Fig. 10 illustrates some polygons for which a correction was needed, together with the final result. Fig. 10a shows a HRU in the Mercier catchment partitioned into pseudo convex units with the centroids completely inside of new ones. Fig. 10b shows a HRU located near the riverside, in which the final units get more regular pieces with a *CI* larger than 0.75. Finally, the resulting polygons in Fig. 10c show that the segmentation process is capable of detecting and segmenting conflictive objects such as "hedges". The *CI* values of all the polygons to be segmented in the Mercier catchment ranged between 0.59 and 0.74. Based on our results, we propose values of *CIT* of 0.75 and 0.88 for simple and detailed meshes respectively.

< Figure 10>

Author-produced version of the article published in Computers & Geosciences, 2013, vol. 57
The original publication is available at http://www.sciencedirect.com/
doi:10.1016/j.cageo.2013.02.006

3.4 Segmentation of very large polygons

26 polygons in the Mercier catchment exceeded an area of 2 ha, the threshold value adopted for the area segmentation. For this process we first subdivided polygons with areas larger than this threshold into TIN's (see Fig. 11a). Then, the routine *Area_segmentation.py* (Table 1) dissolved the triangles using the convexity criterion and the area restriction (see an example of this processes in Fig. 11). After dissolving 165 triangles, we ended up having 17 final homogeneous polygons, all of them with similar areas and a *CI* larger than 0.95, which facilitates running a hydrological model afterwards.

< Figure 11>

3.5 Thresholds and parameter selection to apply GIS tools

The developed computer assisted tools require the definition of the following critical values: (1) In data preparation and cleaning of GIS layers, we selected values of the Snakes elasticity (α = 1.0) and stiffness (β = 1.0), as well as a 50% of points reduction in the Douglas algorithm; (2) threshold values (σ_T) for the standard deviation of properties highly variable within polygons, to separate them into more uniform units. Particularly, for the slope we selected a value of σ_T = 6.0 %; (3) a critical value of the convexity index for the triangulation-dissolution process to remove bad-shaped polygons (i.e. values of 0.75 and 0.88 for simple and detailed meshes respectively); (4) a maximum polygon area (2 ha in the case of the Mercier catchment) to generate a mesh of more homogeneous elements when large polygons due to forest stretches and the low urbanisation occur.

Author-produced version of the article published in Computers & Geosciences, 2013, vol. 57
The original publication is available at http://www.sciencedirect.com/
doi:10.1016/j.cageo.2013.02.006

3.6 Final Improved Mesh

Overall, the mesh improvement produced more HRUs of smaller size, which are more homogeneous and representative of the physical properties within the catchment (see Fig. 7b for the Mercier Catchment). In total, 117 polygons (38.3% of the total catchment area) were treated in the Mercier catchment (i.e. 8 to remove holes, 43 for homogeneity of slopes, 20 to improve convexity, and 46 to reduce area). Thus, the final number of polygons increased from 2,208 to 2,518 in Mercier (14.0 %), and from 2,573 to 2,945 in Chaudanne (14.4 %). For the case of the Mercier catchment, Table 2 shows a reduction in the range of area values, the standard deviation and the mean value for the improved mesh. The minimum value of the *CI* before the improvement (*CI* = 0.599) significantly increases to a value of *CI* = 0.752. Although the average and median values of *CI* changed slightly, the standard deviation of the *CI* values reduced about 20%. Furthermore, the segmentation of the 43 elements with high standard deviation of slope into 133 elements, reduced from 93.4 ha to 51.6 ha the area covered by polygons with highly variable slope, (i.e. from 13% to 7% of the total catchment area). Hence, although the maximum standard deviation increases from 13.98 % to 14.25 % in a HRU unit, the total area of HRUs with non homogeneous representation of slope decreased in 45%. The larger number of polygons in the improved mesh is still compatible with reasonable computing times. The improvement in terms of quality and representation of the HRUs allows obtaining a model mesh more suitable for hydrological modelling.

< Table 2 >

Author-produced version of the article published in Computers & Geosciences, 2013, vol. 57
The original publication is available at http://www.sciencedirect.com/
doi:10.1016/j.cageo.2013.02.006

4. Discussion and interest in terms of hydrological response

The arrangement of the flow paths from the points in the basin to its outlet is of the most crucial importance when studying the structural characteristics of a drainage network, and its implications on the hydrologic response (Rodríguez-Iturbe and Rinaldo, 1997). This is also true for urban catchments (Lhomme et al., 2004; Rodriguez et al., 2003; Rodriguez et al., 2005; Gironás et al., 2007; Gironás et al., 2009; Gironás et al., 2010; Meierdiercks et al., 2010; Rodriguez et al., 2012). Thus, we assessed the effect of the mesh improvement on the generated flow paths by comparing the initial and segmented meshes visually, and by means of the so called width function.

First, we examined the effect of the segmentation procedure on the flow paths linking the polygons. These paths were obtained using the OLAF module (Brossard, 2011, Jankowfsky 2011), which routes the flow between HRUs and the drainage network following topography towards the lowest neighbour HRU or drainage reach. Fig. 12 illustrates some of the major changes both in the extension and trajectory of the flow paths. For example, in the pre-segmented mesh (Fig. 12a), point *a* drains to the stream through point *b*, located north of the stream, which receives contributions from other 3 units. On contrary, a more realistic representation is obtained in the segmented mesh (Fig. 12b), where the flow path starting at the same unit (point *a'*) crosses units *b'* and *c'* before reaching the river at point *d'*. In this case, units *b'* and *c'* are located south of the river. Overall, a denser and potentially more representative network of overland flow paths is observed in the improved mesh, in which the number of HRU's and connections increases (Fig. 12). Indeed, the drainage density of overland flow paths (i.e. the ratio of the total length of the paths

Author-produced version of the article published in Computers & Geosciences, 2013, vol. 57
The original publication is available at http://www.sciencedirect.com/
doi:10.1016/j.cageo.2013.02.006

connecting the HRUs to the catchment area) increased from 19.9 km/km^2 for the pre-segmentation network to 22.4 km/km^2 for the post-segmentation network.

< Figure 12>

We also used the width function $W(x)$ for assessing the effects of segmentation on the organization of the flow paths. $W(x)$ is defined as the number of links at a distance [x, $x+\Delta x$] from the outlet through the drainage network. The linkage between the spatial structure of the basin and its hydrological response is embedded in $W(x)$, because the travel time from each point in the basin is related to the flow velocity and the flow distance that must be covered (Rodríguez-Iturbe and Rinaldo, 1997). $W(x)$ has previously been used to compare drainage network representations (Richards-Pecou, 2002; Moussa, 2008; Rodriguez et al., 2012), and to assess urbanization effects on the drainage network structure and potential impacts in the resulting hydrograph response (e.g., Smith et al., 2002; Gironás et al., 2009; Ogden et al., 2011). Thus, we used $W(x)$ to determine the possible impact of the segmentation procedure in the representation of overland flow paths.

We compared $W(x)$ obtained before and after the mesh segmentation ($W_{pre\text{-}s}(x)$ and $W_{post\text{-}s}(x)$, respectively), using a value of Δx = 20 m (Figure 14a). Our objective was not to quantify the hydrologic effect of the segmentation (a hydrologic model is also required), but to show the effect of different HRU segmentations on the overland flow representation and the generated drainage network. Different networks would have a potential impact on the simulated hydrologic response (i.e. different drainage networks can lead to dissimilar responses using the same hydrological model). We computed the Nash-Sutcliffe (N-S) coefficient, the Modified Efficiency Coefficient (MCE) (Legates and McCabe, 1999) and

Author-produced version of the article published in Computers & Geosciences, 2013, vol. 57
The original publication is available at http://www.sciencedirect.com/
doi:10.1016/j.cageo.2013.02.006

436 the determination coefficient (R^2) to compare $W_{post\text{-}s}(x)$ to $W_{pre\text{-}s}(x)$. Values for these
437 coefficients distinct to one imply differences between both width functions, which also
438 indicate that the terrain before and after the segmentation might also differ hydrologically.
439 In this case both width functions particularly differ at the upper zone of the basin (i.e.
440 distance between 4 400 and 6 000 m from the outlet in Fig. 13a). This difference is strongly
441 associated with the segmentation process, which affects areas located at initial portions of
442 the flow paths.

443 Spectral analysis is a useful tool to study the width function in more details and get
444 information about its structure in the frequency domain (Rodríguez-Iturbe and Rinaldo,
445 1997; Richards-Pecou, 2002; Moussa, 2008). Thus, we further assessed the differences
446 between $W_{pre\text{-}s}(x)$ to $W_{post\text{-}s}(x)$ by comparing the cross-spectral power density between $W_{pre\text{-}}$
447 $_{s}(x)$ and $W_{post\text{-}s}(x)$ (i.e. the power spectral of cross-covariance of the two functions
448 represented by $P_{xy}2$ Fig. 13b), and the power spectral density of $W_{pre\text{-}s}(x)$ (represented by
449 $P_{xy}1$ Fig. 13b). These functions were computed using algorithms embedded in Matlab®.
450 Results demonstrated a significant similitude between $W_{pre\text{-}s}(x)$ and $W_{post\text{-}s}(x)$ at low
451 frequencies, but more noticeable differences at higher frequencies. Thus, large scales
452 features in both cases are very similar (i.e. total area, overall topography and shape, and
453 main channel network structure, etc.), whereas particular features at frequencies higher than
454 0.3/20 m^{-1} = 1/66 m^{-1} are different (i.e. spatial scales smaller than 66 m). The real
455 implications of the differences at these scales between $W_{pre\text{-}s}(x)$ and $W_{post\text{-}s}(x)$ in the
456 simulated hydrologic response should be further studied using a hydrologic model,
457 although noticeable impacts at very small scales are expected. It is also worth noticing that
458 previous studies have concluded that high-frequency components of $W(x)$ may be useful for

Author-produced version of the article published in Computers & Geosciences, 2013, vol. 57
The original publication is available at http://www.sciencedirect.com/
doi:10.1016/j.cageo.2013.02.006

459 classification of river network topology and the regionalization of floods (Richards-Pecou,
460 2002; Lashermes and Foufoula- Georgio, 2007, Moussa, 2008). Finally, and in addition to
461 the hydrologic modelling, in-situ experimental facilities also provide valuable data. In that
462 sense, a dense limnimeter network recently implemented in the Mercier catchment
463 (Sarrazin, 2012), will add valuable information to our results, and help to better understand
464 local hydrological features at these small scales.

465 < Figure 13 >

466 5. Conclusions and Perspectives

467 In this study we proposed and tested various mesh generation tools implemented in
468 GRASS-GIS to improve the HRUs representation used by distributed hydrological models.
469 HRUs can be irregular and numerous for small to medium size catchments, making the
470 computer-assisted pre-processing necessary. The developed algorithms address the
471 following issues to obtain more regular and physically meaningful HRUs:

472 • High heterogeneity in geometric/morphologic properties within the HRUs. We
473 proposed new algorithms for segmentation of units based on DEM-properties,
474 which lead to polygons in which the property is more homogeneous, and therefore
475 more suitable for hydrologic modelling.

476 • Bad shaped polygons. We found that the convexity index was relevant when
477 identifying bad-shaped polygons. These were corrected using a
478 triangulation/dissolution process oriented to increase the convexity index to a value
479 larger than a critical value of 0.75, which we recommended for simple meshes, and
480 0.88 for detailed meshes.

Author-produced version of the article published in Computers & Geosciences, 2013, vol. 57
The original publication is available at http://www.sciencedirect.com/
doi:10.1016/j.cageo.2013.02.006

481 - Very large polygons that transfer large volumes of water into very small units,
482 which can alter the calculation of flow paths, water fluxes and ponding levels. We
483 adopted the segmentation process based on the convexity criterion and a maximum
484 triangular area.

485 Our treatments lead to significant changes both in the extension and trajectory of the
486 overland flow paths. We assessed these changes by comparing the width function before
487 and after processing the mesh representing the terrain. Because of the linkage between this
488 function and the hydrologic response, we concluded that the segmentation processes can
489 impact to some extent in the simulated hydrographs when using a hydrologic model.

490 Potential directions for future research include: (1) generalization and improvement of the
491 sequence in which the mesh segmentation's routines are implemented in order to reduce
492 computation time; (2) implementation of a smoothing process algorithm prior to
493 segmentation to simplify the representation of highly complex polygons in which
494 computation time is very intensive (e.g. polygons created when forest/vegetation
495 representation is too fine); (3) application of the raster property segmentation script with
496 the altitude as criterion given its effect on flow routing; (4) corrections of long and thin
497 HRUs (e.g. roads and hedgerows) by segmentation based on the compact index, as these
498 polygons can act as artificial walls distorting the definition of overland flow paths, despite
499 their high convexity; and (5) use of a hydrologic model to better assess the impacts of the
500 different terrain representations and the segmentation process here proposed on the
501 hydrologic simulation.

502

Author-produced version of the article published in Computers & Geosciences, 2013, vol. 57
The original publication is available at http://www.sciencedirect.com/
doi:10.1016/j.cageo.2013.02.006

503 *ACKNOWLEDGEMENTS*

504 To AVuPUR project funded by the French National Research Agency (contract ANR-07-
505 VULN-01). Data were provided by CCVL, IGN, Grand Lyon, Météo-France, Nantes-
506 Métropole, SAGYRC, SIAVHY, and Sol-Info Rhône-Alpes. SPOT images were acquired
507 thanks to an ISIS contract. We also thank grant No. 11090136 from the Chilean
508 FONDECYT program, financial supports from Irstea-Lyon, through the EGIDE
509 Association, and the Academic Department of University of Chile through its Program of
510 Short Internships.

511

Author-produced version of the article published in Computers & Geosciences, 2013, vol. 57
The original publication is available at http://www.sciencedirect.com/
doi:10.1016/j.cageo.2013.02.006

References

Abbott, M.B., Bathurst, J.C., Cunge, J.A., O'Conell, P.E., Rasmusson, J., 1986a. An introduction to the European Hydrological System-Système Hydrologique Européen, "SHE", 1: History and philosophy of a physically-based distributed modelling system. Journal of Hydrology 87, 45-59.

Abbott, M.B., Bathurst, J.C., Cunge, J.A., O'Connell, P.E., Rasmussen, J., 1986b. An introduction to the European hydrological system — Système Hydrologique Européen "SHE". 2: Structure of a physically-based distributed modelling system. Journal of Hydrology 87, 61-77.

Arnold, J.G., Srinivasan ,R., Muttiah R.S., Williams J.R., 1998. Large area hydrologic modeling and assessment Part I: Model Development. Journal of the American Water Resources Association 34, 73-89.

Beven, K., Kirkby, M.J., 1979. A physically-based variable contributing area model of basin hydrology. Hydrological Sciences Bulletin 24, 43-69.

Bongartz, K., 2003. Applying different spatial distribution and modelling concepts in three nested mesoscale catchments of Germany. Physics and Chemistry of the Earth, Parts A/B/C 28, 1343-1349.

Branger, F., Braud, I., Debionne, S., Viallet, P., Dehotin, J., Hénine, H., Nédélec, Y., Anquetin, S., 2010. Towards multi-scale integrated hydrological models using the LIQUID framework. Overview of the concepts and first application examples. Environmental Modeling & Software 25, 1672-1681.

Author-produced version of the article published in Computers & Geosciences, 2013, vol. 57
The original publication is available at http://www.sciencedirect.com/
doi:10.1016/j.cageo.2013.02.006

Branger, F., Jankowfsky, S., Vannier, O., Viallet, P., Debionne, S., Braud, I., 2012. Use of open-source GIS and data base software for the pre-processing of distributed hydrological models. In: Bocher, E., Neteler, M. (Eds). Geospatial Free and Open Source Software in The 21rst Century, Lecture notes in Geoinformation and Cartography, Springer, Berlin, pp. 35-48.

Braud, I., Breil, P., Thollet, F., Lagouy, M., Branger, F., Jacqueminet, C., Kermadi, S., Michel, K., 2012. Evidence of the impact of urbanization on the hydrological regime of a medium-sized periurban catchment in France, Journal of Hydrology, in press. doi: 10.1016/j.jhydrol.2012.04.049.

BRGM, 2013. Bureau of Geological and Mining Research. URL:http://infoterre.brgm.fr/viewer/MainTileForward.do;jsessionid=C6247604415C79ABC4729563FD5969E, [In French, accessed 29 January 2013]

Bocher, E., Martin, J.Y., 2012. TAnaTo2: A Tool to Evaluate the Impact of Natural and Anthropogenic Artefacts with a TIN-Based Model. In: Bocher, E., Neteler, M. (Eds). Geospatial Free and Open Source Software in The 21rst Century, Lecture notes in Geoinformation and Cartography, Springer, Berlin, pp. 63-85.

Brossard, F., 2011. Automatisation du prétraitement des données spatiales pour la modélisation hydrologique distribuée en zone péri-urbaine (Automatic preprocessing of spatial data for a distributed hydrological modeling in a peri-urban zone). Rapport de Stage 2AE. EPMI École D'Ingenieurs, Cemagref-Lyon, pp. 77 [in French].

CGAL, 2011. Computational Geometry Algorithms Library (CGAL). URL: www.cgal.org (accessed 29 January 2013).

555 Dehotin, J., Braud, I., 2008. Which spatial discretization for distributed hydrological
556 models? Proposition of a methodology and illustration for medium to large scale
557 catchments. Hydrology and Earth System Sciences 12, 769-796.

558 Di Luzio, M., Srinivasan, R., Arnold, J.G., 2004. A GIS-Coupled Hydrological Model
559 System for the Watershed Assessment of Agricultural Nonpoint and Point Sources of
560 Pollution. Transactions in GIS 8, 113–136.

561 Douglas, D.H., Peucker, T.K., 1973. Algorithms for the reduction of the number of points
562 required to represent a digitized line or its caricature. Cartographica: The International
563 Journal for Geographic Information and Geovisualization 10, 112-122.

564 Flügel, W.A., 1995. Delineating hydrological response units by geographical information
565 system analyses for regional hydrological modelling using PRMS/MMS in the
566 drainage basin of the River Bröl, Germany. Hydrological Processes 9, 423-436.

567 Garbrecht, J., Martz, L.W., 1997. TOPAZ version 1.20: An automated digital landscape
568 analysis tool for topographic evaluation, drainage identification, watershed
569 segmentation and subcatchments parametrization – Overview. In: Rep.# GRL 97-2.
570 Grazinglands Research Laboratory, USDA, Agricultural Research Service, El Reno,
571 OK, 21 pp.

572 Gironás, J., Andrieu, H., Roesner, L., 2007. Alterations to Natural Catchments due to
573 Urbanization, a Morphologic Approach. In: GRAIE, Lyon, France (Ed). Novatech
574 2007, Section 6.2, pp. 1199-1206.

Author-produced version of the article published in Computers & Geosciences, 2013, vol. 57
The original publication is available at http://www.sciencedirect.com/
doi:10.1016/j.cageo.2013.02.006

Gironás, J., Niemann, J.D., Roesner, L.A., Rodriguez, F., Andrieu, H., 2009. A morpho-climatic instantaneous unit hydrograph model for urban catchments based on the kinematic wave approximation. Journal of Hydrology 377, 317-334.

Gironás, J., Niemann, J.D., Roesner, L.A., Rodriguez, F., Andrieu, H., 2010. Evaluation of methods for representing urban terrain in stormwater modeling. Journal of Hydrologic Engineering 15, 1-14.

GRASS Development Team, 2011. Geographic Resources Analysis Support System (GRASS) Software. Open Source Geospatial Foundation Project. URL: http://grass.osgeo.org (accessed 29 January 2013).

Greene, D., 1983. The decomposition of polygons into convex parts. Computational Geometry 1, 235-259.

Hertel, S., Mehlhorn, K., 1983. Fast triangulation of simple polygons. In: Karpinski, M. (Eds). Proceedings 4th International Conference Foundations Computation Theory, Lecture Notes in Computer Science, Vol. 158, pp. 207-218.

Hofierka, J., Mitasova, H., Neteler, M., 2007. Terrain parameterization in GRASS. In Geomorphometry. In: Hengl, T., Reuter, H.I. (Eds), Geomorphometry: Concepts, Software, Applications. Developments in Soil Science, Elsevier, Vol. 33, 1-28 pp.

IGCS, 2013. Inventaire et Gestion des Sols, http://www.gissol.fr/programme/igcs/rrp.php (accessed January 30 2013)

Ivanov, V.Y., Vivoni, E.R., Bras, R.L., Entekhabi, D., 2004. Catchment hydrologic response with a fully distributed triangulated irregular network model. Water Resource Research 40, W11102, doi: 10.1029/2004WR003218.

Jacqueminet, C., Kermadi, S., Michel, K., Béal, D., Branger, F., Jankowsky, S., Braud, I., 2013. Land cover mapping using aerial and VHR satellite images for distributed hydrological modelling of periurban catchments: application to the Yzeron catchment (Lyon, France). Journal of Hydrology, in press, DOI 10.1016/j.jhydrol.2013.01.028 .

Jankowfsky, S., Branger, F., Braud, I., Debionne, S., Viallet, P., Rodriguez, F., 2010. Development of a suburban catchment model within the LIQUID® framework. In: Proceedings of the International congress on Environmental Modelling and Software, iEMSs 2010, Ontario, Ottawa, Canada, pp. 9.

Jankowfsky, S., Branger, F., Braud, I., Gironás, J., Rodriguez, F., 2012. Comparison of catchment and network delineation approaches in complex suburban environments. Application to the Chaudanne catchment, France. Hydrological Processes. In press. doi: 10.1002/hyp.9506

Jankowfsky, S., 2011. Understanding and modelling of hydrological processes in small peri-urban catchments using an object oriented and modular distributed approach. Application to the Chaudanne and Mercier sub-catchments (Yzeron Catchment, France). École Doctorale Terre, Univers, Environnement. l'Institut National Polytechnique de Grenoble. URL : http://tel.archives-ouvertes.fr/tel-00721988 (accessed 29 January 2013).

615 Kass, M., Witkin, A., Terzopoulos, D., 1988. Snakes: Active Contour Models. International
616 Journal of Computer Vision 1, 321-331.

617 Klingseisen, B., Metternicht, G., Paulus, G., 2008. Geomorphometric landscape analysis
618 using a semi-automated GIS-approach. Environmental Modelling & Software 23(1),
619 109–121.

620 Krause P., 2002. Quantifying the impact of land use changes on the water balance of large
621 catchments using the J2000 model. Physics and Chemistry of the Earth 27, 663–673.

622 Lashermes, B., Foufoula-Georgiou, E., 2007. Area and width functions of river networks:
623 New results on multifractal properties. Water Resources Research 43, W09405,
624 doi:10.1029/2006WR005329.

625 Lagacherie, P., Rabotin, M., Colin, F., Moussa, R., Voltz, M., 2010. Geo-MHYDAS: A
626 landscape discretization tool for distributed hydrological modeling of cultivated areas.
627 Computers & Geosciences 36, 1021-1032.

628 Legates, D.R., McCabe Jr., G.J., 1999. Evaluating the use of "goodness-of-fit" measures in
629 hydrologic and hydroclimatic model validation. Water Resources Research 35, 233-
630 241. doi:10.1029/1998WR900018.

631 Lhomme, J., Bouvier, C., and Perrin, J. L., 2004. Applying a GIS-based geomorphological
632 routing model in urban catchments. Journal of Hydrology 299(3-4), 203–216.

633 Meierdiercks, K.L., Smith, J.A., Baeck, M.L. Miller, A.J., 2010. Analyses of urban
634 drainage network structure and its impact on hydrologic response. Journal of the
635 American Water Resources Association 46, 932–943.

636 Moussa, R., 2008. What controls the width function shape, and can it be used for channel
637 network comparison and regionalization? Water Resources Research 44: W08456,
638 doi:10.1029/2007WR006118.

639 Moussa, R., Voltz, M., Andrieux, P., 2002. Effects of the spatial organization of
640 agricultural management on the hydrological behaviour of a farmed catchment during
641 flood events. Hydrological Processes 16, 393-412.

642 Ogden, F.L., Raj Pradhan, N., Downer, C.W., Zahner, J.A., 2011. Relative importance of
643 impervious area, drainage density, width function, and subsurface storm drainage on
644 flood runoff from an urbanized catchment. Water Resources Research 47, W12503,
645 doi: 10.1029/2011WR010550.

646 Olivera, F., Furnans, J., Maidment, D.R., Djokic, D., Ye, Z., 2002. Drainage systems. Arc
647 Hydro, GIS for water resources, D. R. Maidment, ed., ESRI, Redlands, Ca, 55-86.

648 O'Rourke, J., 1998. Computational Geometry in C, 2nd edition. Cambridge University
649 Press, Cambridge, England, 376 pp.

650 Python Software Foundation, 2011. Python Programming Language – Official Website.
651 URL:www.python.org (accessed 29 January 2013)

652 R Development Core Team, 2011. R: A language and environment for statistical
653 computing. R Foundation for Statistical Computing, Vienna, Austria.
654 URL: http://www.R-project.org/ (accessed 29 January 2013).

655 Rabotin M., 2010. General Manual GeoMhydas. Laboratory of Interactions Soil -
656 Agrosystem - Hydrosytem (LISAH), Montpellier, France. URL: http://www.umr-

657 lisah.fr/openfluid/index.php?page=dloadsmhy&lang=en&part=mhydas (accessed 29
658 January 2013).

659 Richards-Pecou, B., 2002. Scale invariance analysis of channel network width function and
660 possible implications for flood behaviour. Hydrological Sciences Journal 47(3), 387–
661 404.

662 Rodriguez, F., Andrieu, H., Creutin, J., 2003. Surface runoff in urban catchments:
663 morphological identification of unit hydrographs from urban databanks. Journal of
664 Hydrology 283, 146-168.

665 Rodriguez, F., Cudennec, C., Andrieu, H., 2005. Application of morphological approaches
666 to determine unit hydrographs of urban catchments. Hydrological Processes 19(5),
667 1021–1035.

668 Rodriguez, F., Bocher, E., Chancibault, K., 2012. Terrain representation impact on
669 periurban catchment morphological properties, Journal of Hydrology. In press. doi:
670 10.1016/j.jhydrol.2012.11.023.

671 Rodriguez-Iturbe, I., Rinaldo, A., 1997. Fractal River Basins: Chance and Self-
672 organization. Cambridge University Press, New York, 564 pp.

673 Russ, J.C. 2002. The Image Processing Handbook. Fourth edition. CRC Press, Boca Raton,
674 EUA, 732 pp.

675 Sarrazin, B., 2012. MNT et observations multi-locales du réseau hydrogranphique d'un
676 petit bassin versant rural dans une perspective d'aide à la modélisation hydrologique.
677 (DTM and local observations of the river network of a small rural catchment with a

678 view to support hydrological modelling). Ph.D. Dissertation, École Doctorale Terre,
679 Univers, Environnement. l'Institut National Polytechnique de Grenoble, 275 pp [in
680 French].

681 Seyfried, M., Wilcox, B., 1995. Scale and the nature of spatial variability: field examples
682 having implications for hydrologic modeling. Water Resources Research 31, 173-184.

683 Schwartze, C., 2008. Deriving Hydrological Response Units (HRUs) using a Web
684 Processing Service implementation based on GRASS-GIS. In: Geoinformatics FCE
685 CTU 2008. Workshop Proceedings, Vol. 3, pp. 67-78.

686 Shewchuck J., 1996. Triangle: Engineering a 2D Quality Mesh Generator and Delaunay
687 Triangulator. In: Lin, M., Manocha, D., (Eds), Applied Computational Geometry:
688 Towards Geometric Engineering, Vol. 1148, pp. 203-222.

689 Smith, J., Lynn, M., Morrison, J. Sturdevant-Rees, P., Turner-Guillespie, D., Bates P.,
690 2001. The regional hydrology of extreme floods in an urbanizing drainage basin.
691 Journal of Hydrometeorology 3, 267-282.

692 Taylor, J. A., Coulouma, G., Lagacherie, P., Tisseyre, B., 2009. Mapping soil units within a
693 vineyard using statistics associated with high-resolution apparent soil electrical
694 conductivity data and factorial discriminant analysis. Geoderma 153(1-2), 278-284.

695 VanderKwaak, J.E., Loague, K., 2001. Hydrologic-response simulations for the R-5
696 catchment with a comprehensive physics-based model. Water Resources Research
697 37(4), 999-1013.

Author-produced version of the article published in Computers & Geosciences, 2013, vol. 57
The original publication is available at http://www.sciencedirect.com/
doi:10.1016/j.cageo.2013.02.006

698 Viviroli, D., Zappa, M., Gurtz, J., Weingartner, R., 2009. An introduction to the
699 hydrological modelling system PREVAH and its pre- and post-processing tools.
700 Environmental Modelling and Software 24, 1209–1222.

701 Wolock, D.M., Price, C.V., 1994. Effects of digital elevation model map scale and data
702 resolution on a topography-based watershed model. Water Resource Research 30,
703 3041-3052.

704 Zhang, W., Montgomery, D., 1994. Digital elevation model grid size, landscape
705 representation, and hydrologic simulations. Water Resource Research 30, 1019-1028.

706

Author-produced version of the article published in Computers & Geosciences, 2013, vol. 57
The original publication is available at http://www.sciencedirect.com/
doi:10.1016/j.cageo.2013.02.006

Appendices

Appendix A.1.: Raster-property segmentation script

1.-Extract the raster property with the polygon mask

2.-Get property statistics for each polygon (average, standard deviation) (Fig. 3a)

3.-If $\sigma > \sigma_T$

4.- Get Q1 and Q3 quartile values in the raster map

5.- Create Contour polylines with Q1 and Q3 values classification (Fig. 3c)

6.- Dissolve small areas and preserve only the three largest areas (Fig. 3c)

7.- Smooth Contours with Snakes Algorithm (Fig. 3d)

8.- Reduce vertex Contours with Douglas-Peucker Algorithm (Fig. 3e)

9.- Split Polygon with Q1 and Q3 contour polyline (Fig. 3f)

Author-produced version of the article published in Computers & Geosciences, 2013, vol. 57
The original publication is available at http://www.sciencedirect.com/
doi:10.1016/j.cageo.2013.02.006

719 Appendix A.2.: Convex segmentation script

720 1.- For each polygon P with CI ≤ CIT

721 2.- Apply Triangle

722 3.- While P has triangles not yet dissolved

723 4.- Select triangle with the largest area

724 5.- Select triangle neighbour with the largest area and create new group P'

725 6.- While C. I. of P' ≥ CIT

726 7.- Search the neighbour triangles with the largest area

727 8.- Dissolve boundaries of this group

728 9.- Compute the CI of this new group

729 10.- end while

730 11.- Update P = P – P'

731 12.- end While

732 13.- Dissolve areas < area threshold

733 14.- end For

734

735

Author-produced version of the article published in Computers & Geosciences, 2013, vol. 57
The original publication is available at http://www.sciencedirect.com/
doi:10.1016/j.cageo.2013.02.006

List of Figures

Author-produced version of the article published in Computers & Geosciences, 2013, vol. 57
The original publication is available at http://www.sciencedirect.com/
doi:10.1016/j.cageo.2013.02.006

754 Figure 9: HRU's examples from the Chaudanne catchment: (a) two holes produced by
755 green areas, (b) one hole produced by green area, (c) one hole produced by a manmade
756 feature.

757 Figure 10: Examples of HRUs segmented using a *CIT* = 0.75.

758 Figure 11: Example of segmentation of very large polygons: (a) Triangulated large
759 polygon: 19.2 ha, and (b) dissolved homogeneous polygons with CIT $\geq$ 0.95 and area $\geq$ 2
760 ha.

761 Figure 12: Generated overland flow paths in the Mercier Catchment: (a) pre-segmented
762 mesh, (b) post-segmented mesh.

763 Figure 13: (a) Width function W(x) of Mercier Drainage Network for the pre- and the post-
764 segmentation (b) Power spectral density of Wpre-s(x), Pxy1, and Cross-spectral power
765 density between Wpre-s(x) and Wpost-s(x), Pxy2.

766

767 List of Tables

771

Author-produced version of the article published in Computers & Geosciences, 2013, vol. 57
The original publication is available at http://www.sciencedirect.com/
doi:10.1016/j.cageo.2013.02.006

772 Table 1: Summary of the different tasks and scripts developed.

Task	Description	Script developed
Partition of polygons with holes	***Data preparation and cleaning of GIS layers:*** Split polygons and create a new subset without holes.	Polygons_Holes.py
Integration of raster based properties into polygons	***Segmentation of polygons with high variability of a raster based property:*** Segmentation with Inter Quartile Range (IQR) boundaries and small area dissolving. Final smoothing with Snakes algorithm and reduction of vertexes with Douglas algorithm.	Slope_Segmentation.py
Convexity Segmentation	***Removal of bad-shaped polygons:*** Triangulation with Software Triangle. Exporting and Importing GRASS ASCII into POLY format with R Script. Dissolving rule with Convexity Index criterion.	Convexity_Segmentation.py Ascii2Poly.r Triangle2Ascii.r
Area Segmentation	***Segmentation of too large polygons:*** Idem to Convexity Segmentation but with additional restriction of maximum area in initial triangulation. Dissolving Rule with Convexity Index and Area restriction.	Area_Segmentation.py

773

774

Author-produced version of the article published in Computers & Geosciences, 2013, vol. 57
The original publication is available at http://www.sciencedirect.com/
doi:10.1016/j.cageo.2013.02.006

775 Table 2: Main statistics of Area and Convexity Index in the Mercier catchment for the Initial and

776 Optimized Mesh.

	Area (m^2)		Standard deviation of Slope (%)		Convexity Index	
	Initial Mesh	Optimized Mesh	Initial Mesh	Optimized Mesh	Initial Mesh	Optimized Mesh
Average	3 289	2 899	3.09	3.14	0.969	0.974
Median	834	945	2.58	2.64	0.990	0.991
Min	2	10	0.12	0.12	**0.599**	**0.752**
Max	**192 144**	**24 595**	13.98	14.25	1.000	1.000
Std	8 270	4 461	2.16	2.18	0.052	0.040

777

778

779

780

Author-produced version of the article published in Computers & Geosciences, 2013, vol. 57
The original publication is available at http://www.sciencedirect.com/
doi:10.1016/j.cageo.2013.02.006

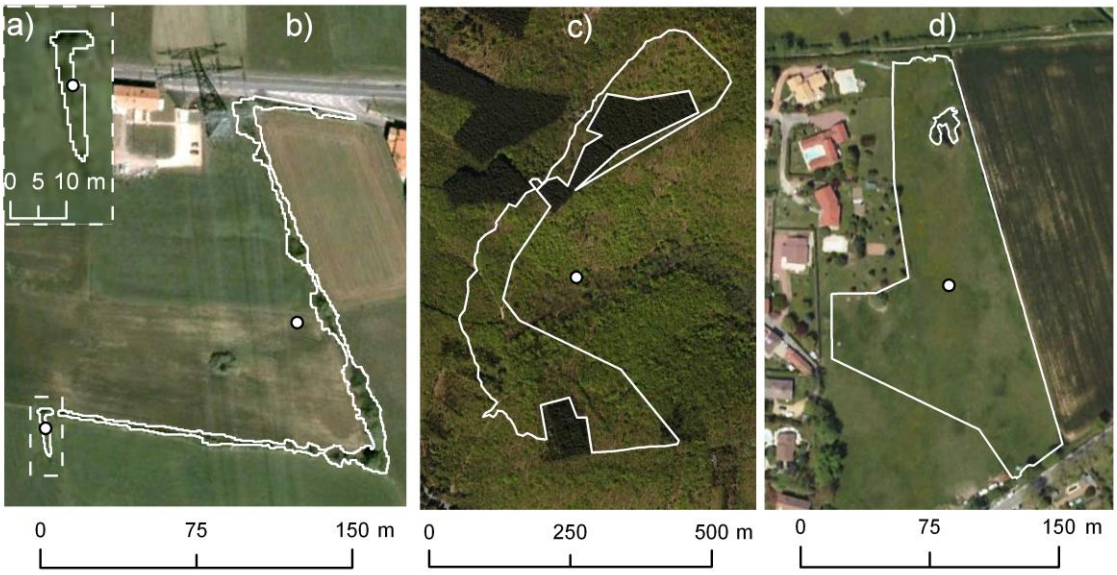

781

782 Figure 1

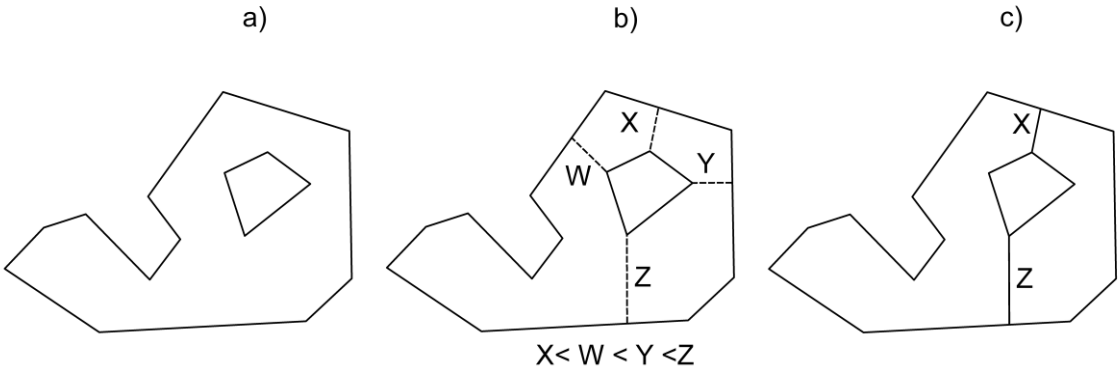

783

784 Figure 2

785

786

Author-produced version of the article published in Computers & Geosciences, 2013, vol. 57
The original publication is available at http://www.sciencedirect.com/
doi:10.1016/j.cageo.2013.02.006

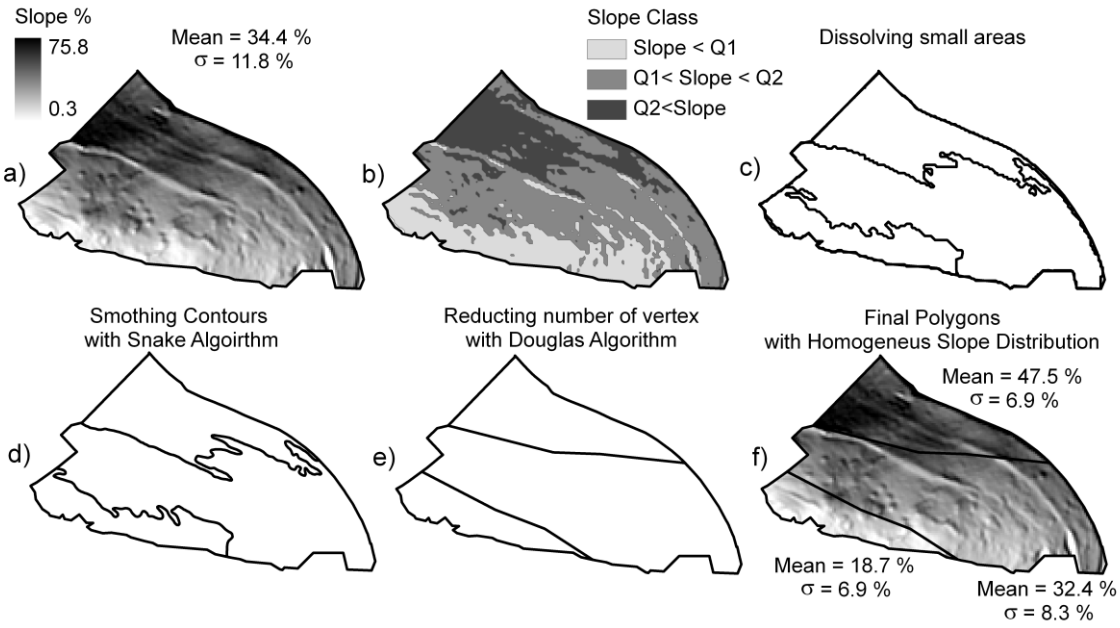

787

788 Figure 3

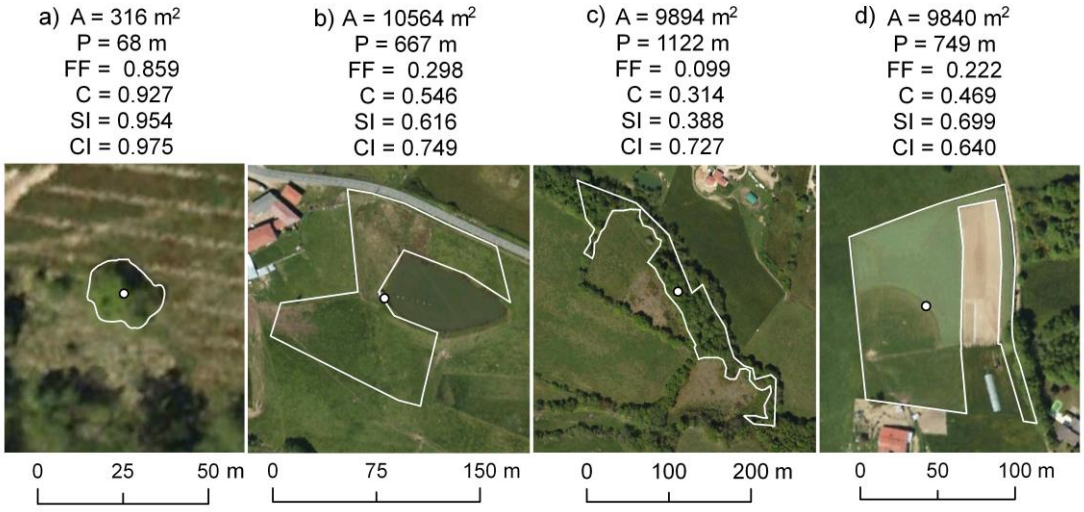

789

790 Figure 4

791

Author-produced version of the article published in Computers & Geosciences, 2013, vol. 57
The original publication is available at http://www.sciencedirect.com/
doi:10.1016/j.cageo.2013.02.006

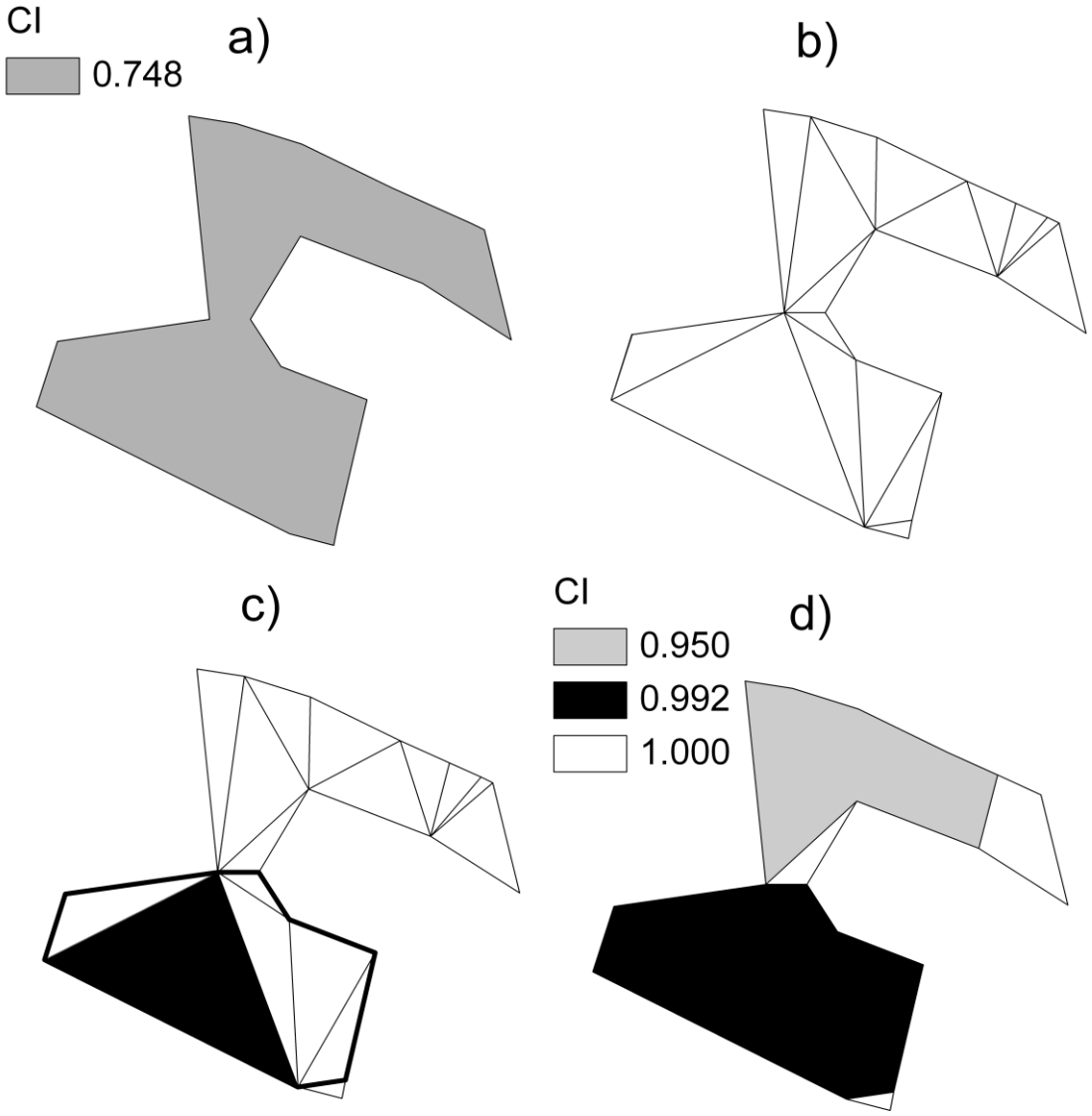

792

793 Figure 5

794

Author-produced version of the article published in Computers & Geosciences, 2013, vol. 57
The original publication is available at http://www.sciencedirect.com/
doi:10.1016/j.cageo.2013.02.006

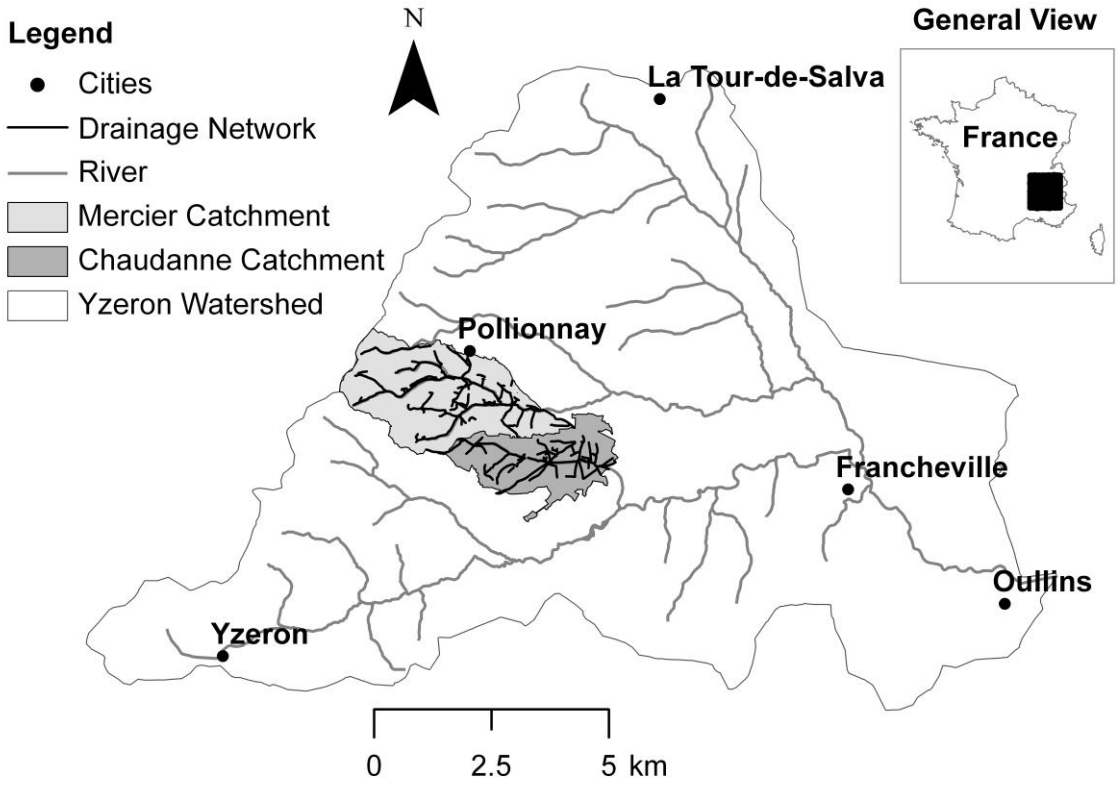

795

796 Figure 6

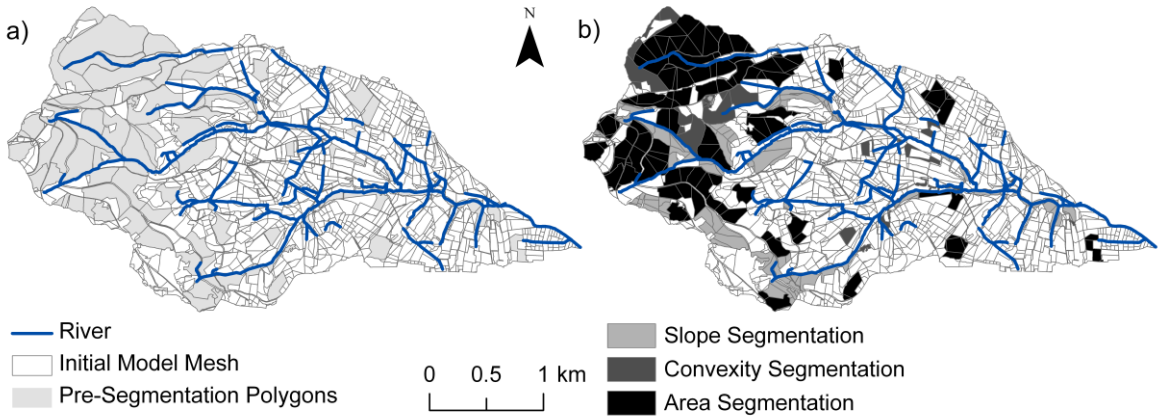

797

798 Figure 7

799

Author-produced version of the article published in Computers & Geosciences, 2013, vol. 57
The original publication is available at http://www.sciencedirect.com/
doi:10.1016/j.cageo.2013.02.006

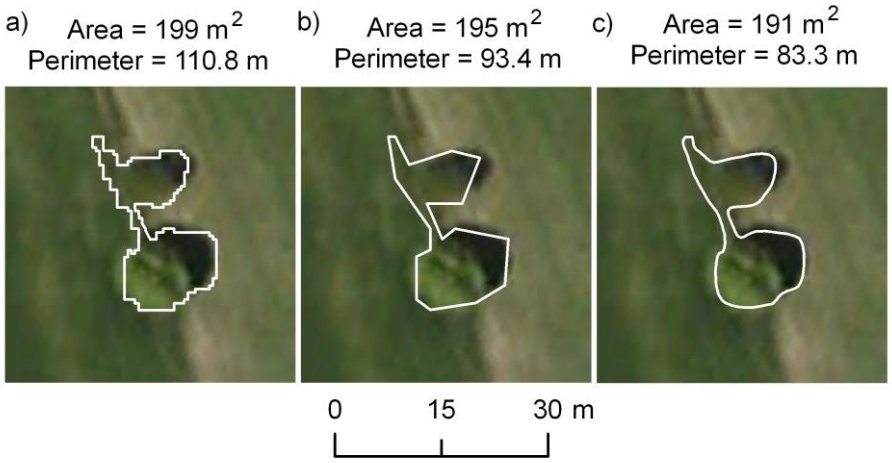

800

801 Figure 8

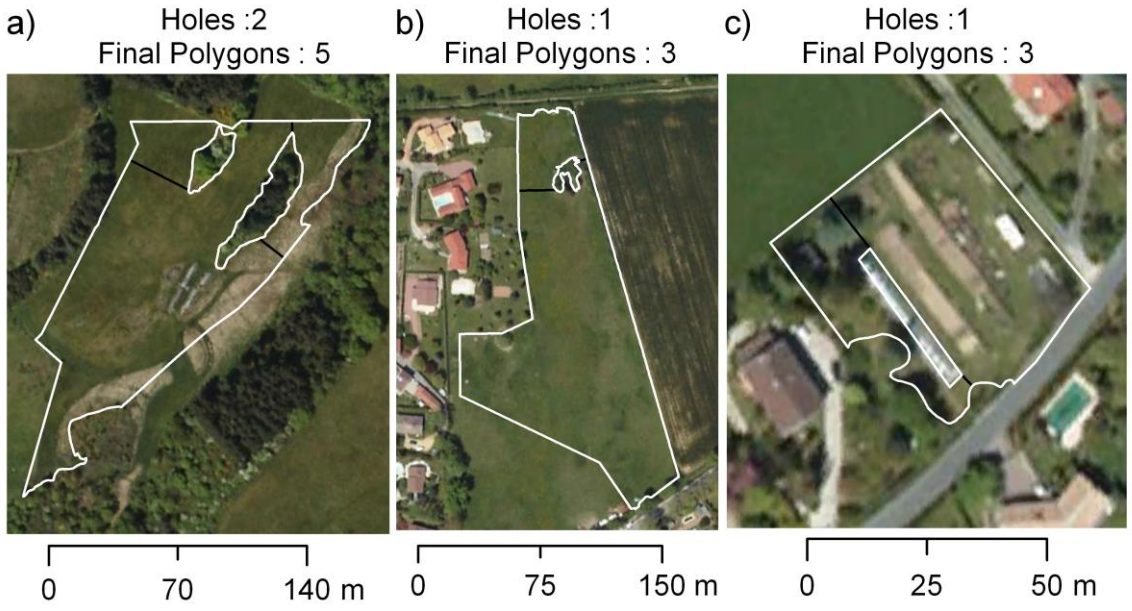

802

803 Figure 9

804

Author-produced version of the article published in Computers & Geosciences, 2013, vol. 57
The original publication is available at http://www.sciencedirect.com/
doi:10.1016/j.cageo.2013.02.006

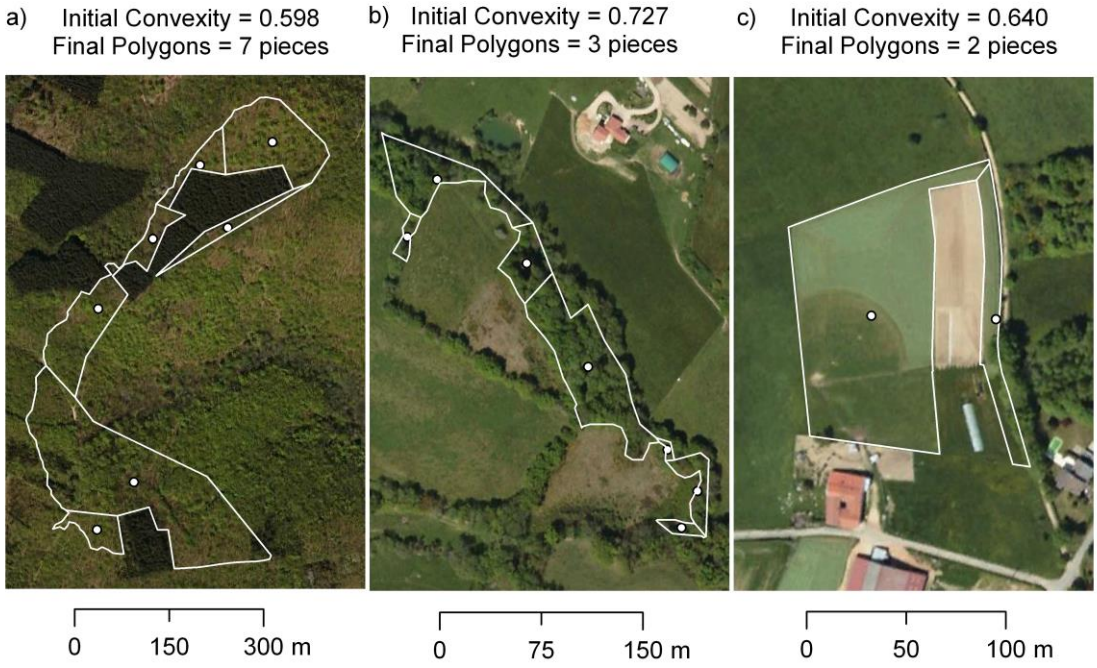

805

806 Figure 10

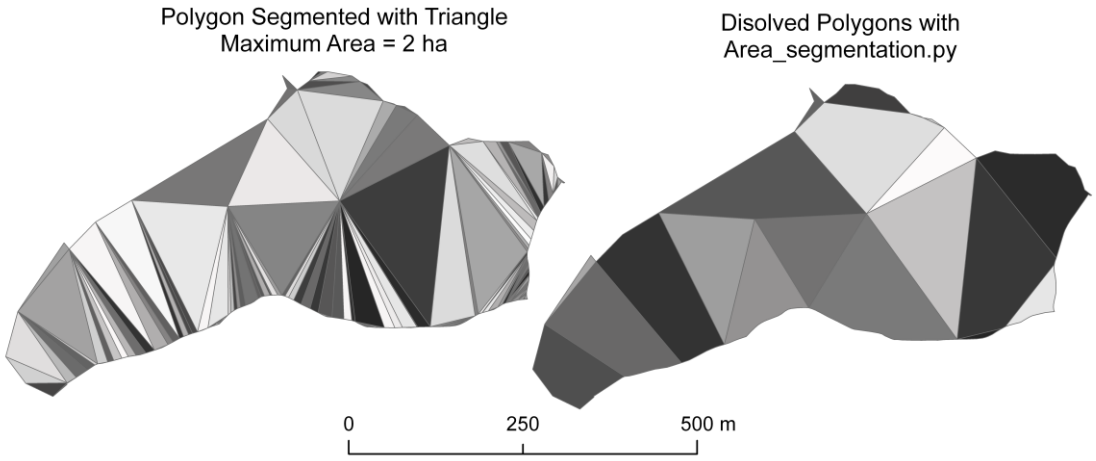

807

808 Figure 11

809

Author-produced version of the article published in Computers & Geosciences, 2013, vol. 57
The original publication is available at http://www.sciencedirect.com/
doi:10.1016/j.cageo.2013.02.006

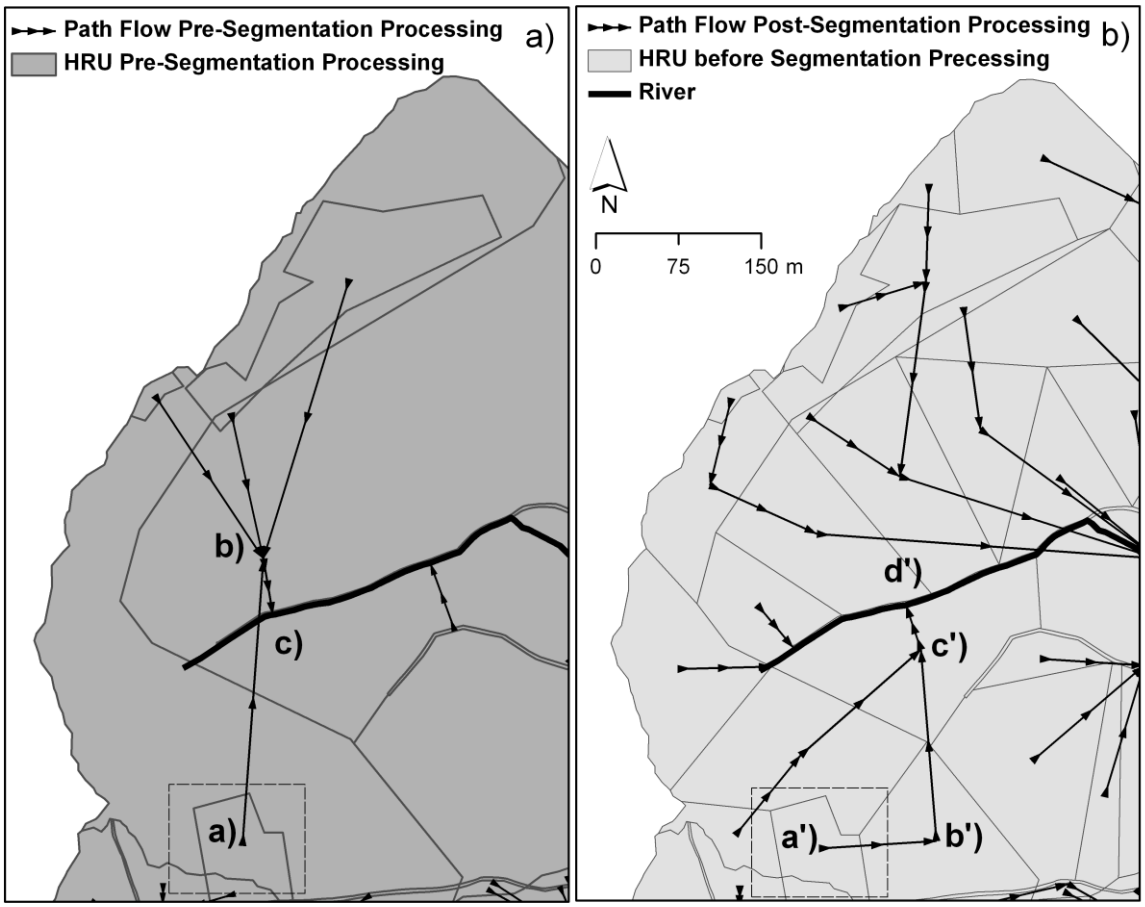

Figure 12

Author-produced version of the article published in Computers & Geosciences, 2013, vol. 57
The original publication is available at http://www.sciencedirect.com/
doi:10.1016/j.cageo.2013.02.006

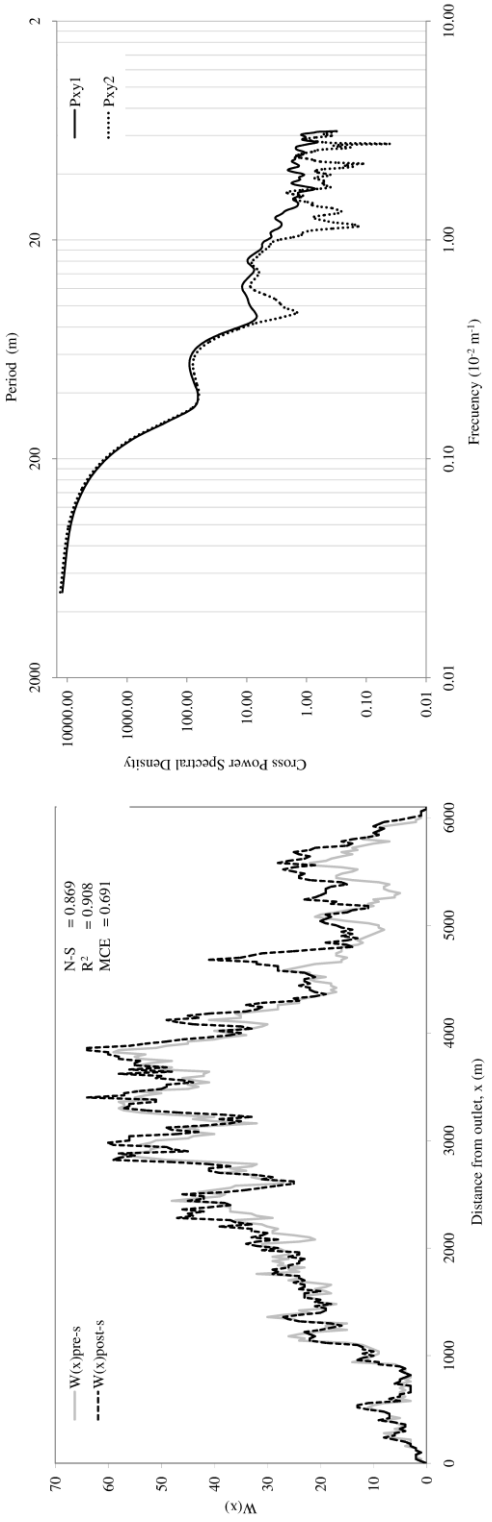

Figure 13